JOC The Journal of Organic Chemistry

Article

pubs.acs.org/joc

# The Leaving Group Strongly Affects $H_2O_2$-Induced DNA Cross-Linking by Arylboronates

Sheng Cao,‡ Yibin Wang,‡ and Xiaohua Peng*

Department of Chemistry and Biochemistry, University of Wisconsin—Milwaukee, 3210 North Cramer Street, Milwaukee, Wisconsin 53211, United States

Supporting Information

**ABSTRACT:** We evaluated the effects of the benzylic leaving group and core structure of arylboronates on $H_2O_2$-induced formation of bisquinone methides for DNA interstrand cross-linking. The mechanism of DNA cross-linking induced by these arylboronates involves generation of phenol intermediates followed by departure of benzylic leaving groups leading to QMs which directly cross-link DNA via alkylation. The QM formation is the rate-determining step for DNA cross-linking. A better leaving group (Br) and stepwise bisquinone methide formation increased interstrand cross-linking efficiency. These findings provide essential guidelines for designing novel anticancer prodrugs.

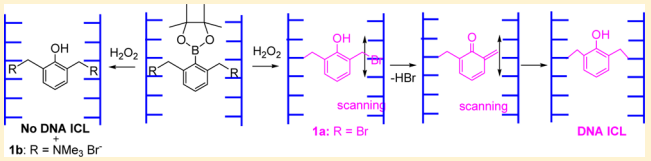


## INTRODUCTION

Interest in the development of cancer therapies with improved selectivity and reduced host toxicity has been growing.[1−3] One effective approach is to design prodrugs that can be activated under tumor-specific conditions.[4] Tumor cells produce high levels of reactive oxygen species (ROS), which makes them distinctly different from normal cells.[5−7] Taking advantage of this difference, our group recently developed a novel prodrug strategy involving $H_2O_2$-induced DNA cross-linking by a nitrogen mustard cytotoxin for the selective destruction of tumor cells.[8] Quinone methides (QMs) are the ultimate cytotoxins responsible for the activities of many anticancer drugs.[9,10] Therefore, the development of prodrugs that can be activated under tumor-specific conditions to form QMs is a promising approach for the targeted destruction of tumor cells. Various methods have been developed for QM formation, such as photoirradiation, oxidation, thermal extrusion reactions, acid- or base-facilitated reactions, and fluoride- or $H_2O_2$-induced reactions.[10−19] However, most of these methods have disadvantages, including the inaccessibility of precursors, undesirably high reaction temperatures, long reaction times, the requirement for additional reagents and acidic or basic conditions, and the occurrence of various side reactions.[20] Compared with these other methods, $H_2O_2$-induced QM generation from arylboronates is more attractive for in vivo applications because $H_2O_2$-induced cleavage of boronate esters is a bioorthogonal reaction and $H_2O_2$ is bioavailable.

Previously, we reported that arylboronic ester quaternary ammonium salt **4b** can be activated by $H_2O_2$ to generate a bisQM that forms DNA interstrand cross-links (ICLs).[13] In contrast, QMs are not generated from arylboronic esters **2b** and **3b**, which have similar structures. Preliminary mechanistic studies showed that the structure of the aromatic core, the chemical properties of the benzylic leaving group, and the aromatic substituents affect QM formation.[13,21] Inspired by these findings, we synthesized three new arylboronic esters (**1a**, **1b**, and **4c**) in this study and used **1**−**4** to conduct a more-detailed investigation of the effects of the leaving group and the aromatic core structure on the DNA cross-linking ability of these arylboronic esters.

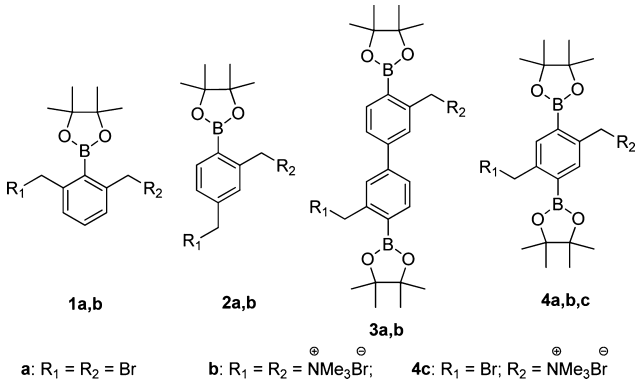


## RESULTS AND DISCUSSION

Compound **1a** was synthesized starting from 2-bromo-*m*-xylene (**5**) via palladium-catalyzed borylation followed by bromination (Scheme 1). Quaternization of **1a** with trimethylamine provided **1b** in nearly quantitative yield. Compounds **2**−**4** were synthesized as previously described.[13]

We investigated the DNA cross-linking abilities of **1**−**4** by allowing them to react with 49-mer DNA duplex **7** in a phosphate buffer at 37 °C for 24 h for **1a**−**4a** or 48 h for **1b**−**4b** (Scheme 2). ICL formation and yields were analyzed via denaturing polyacrylamide gel electrophoresis with phosphor image analysis. Efficient ICL formation was observed with

**Received:** August 27, 2013
**Published:** December 30, 2013

**Scheme 1. Synthesis of 1a and 1b**

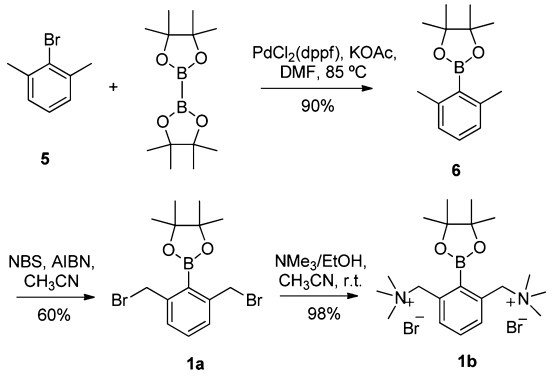


bromide **1a** (cross-linking yield 25%) but not with the corresponding quaternary ammonia salt **1b** (0%; Figure 1, compare lanes 3 and 7). To determine the generality of this leaving-group effect, we investigated the cross-linking abilities of **2a**,**b** and **3a**,**b** and found that, like **1a**, bromides **2a** (24%) and **3a** (9%) efficiently induced DNA cross-linking, whereas quaternary ammonia salts **2b** and **3b** did not (Figure 1, compare lanes 4 and 5 to lanes 8 and 9, respectively). Bromine, which is a better leaving group than trimethylamine, greatly improved the cross-linking yield. The cross-linking efficiencies of compounds **1a**−**3a** were affected by their concentrations, the compound/$H_2O_2$ ratios, and the pH of the buffer solution (Supporting Information, Figures S1 and S2). The best compound/$H_2O_2$ ratios were 2:1 for **1a** and **2a** and 1:1 for **3a**. Cross-linking yields for **1a**−**3a** were lower under acidic conditions than under basic conditions (Supporting Information, Figure S2). These results are consistent with previously reported results.[13]

Surprisingly, the quaternary ammonia salt **4b**, the core structure of which bears two boronate groups, showed a higher cross-linking yield (23%) than the corresponding bromide **4a** (3.5%; Figure 1, compare lanes 10 and 6), perhaps because **4b** is more water-soluble than **4a**. In fact, **4a** precipitated from the reaction mixture. In order to test our hypothesis, we synthesized compound **4c** containing a mixed leaving group, Br and $NMe_3$ (Scheme 3), and investigated its cross-linking ability. Compound **4c** is completely dissolved in water or a mixture of $H_2O/CH_3CN$. Precipitation was not observed during the cross-linking reaction. As we expected, compound **4c** displayed a much higher cross-linking yield (33.7%; Figure 1, lane 11) than the bromide **4a** (3.5%) and the quaternary ammonia salt **4b** (23.0%) under the same incubation conditions. The result suggested that in addition to the leaving groups the water solubility also affects the cross-linking efficiency of **4a**−**c**.

We further explored the reactivities of bromides **1a**−**4a** by determining the heat stability of purified cross-linked products and monoalkylated single-stranded DNA. About 55−62% of

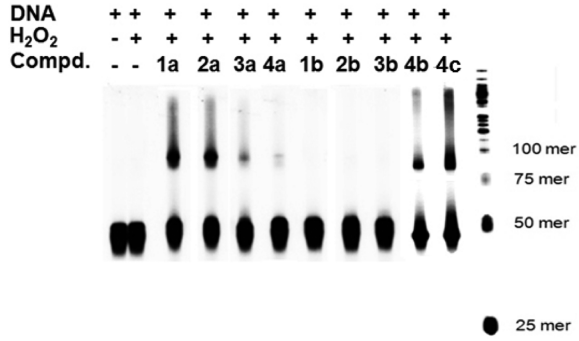


**Figure 1.** $H_2O_2$-induced DNA ICL formation by compounds **1**−**4**. Lane 1: DNA only (cross-linking yield 0%). Lane 2: DNA with 100 $\mu$M $H_2O_2$ (0%). Lane 3: 2 mM **1a** (25%). Lane 4: 2 mM **2a** (24%). Lane 5: 2 mM **3a** (9%). Lane 6: 2 mM **4a** (3.5%). Lane 7: 2 mM **1b** (0%). Lane 8: 2 mM **2b** (0%). Lane 9: 2 mM **3b** (0%). Lane 10: 2 mM **4b** (23%). Lane 11: 2 mM **4c** (33.7%). Lane 12: DNA marker; [$H_2O_2$] = 1 mM for **1**, **2**, and **4**, and 2 mM for **3**. (Reaction mixture was incubated at 37 °C for 48 h.)

**Scheme 3. Synthesis of 4c That Contains Mixed Leaving Groups**

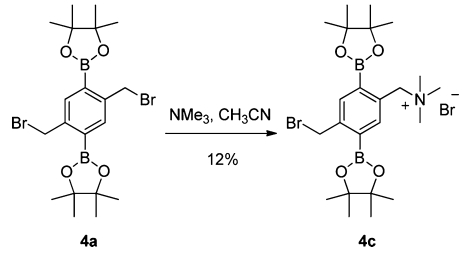


the ICLs formed from **1a**−**4a** were stable to heating in phosphate buffer. Obvious cleavage bands were observed with dGs upon heating in 1.0 M piperidine (Figure 2 and Supporting Information, Figures S3−S5), which is known to induce cleavage of N-7-alkylated purines upon heating.[22,23] Clearly, the cross-linking reactions occurred mainly with dGs. To confirm this, we synthesized two DNA duplexes with different sequences (**8** and **9**, Scheme 2). Duplex **9** contains self-complementary dAT sequences, whereas **8** contains dCs/dTs in one strand and dGs/dAs in the other strand. ICLs were not observed when **9** was treated with **1a**−**4a**, which suggests that cross-linking reactions did not take place with dT and dA (Supporting Information, Figure S6). However, **1a**−**4a** did induce ICL formation with duplex **8** (2−12%, Supporting Information, Figure S7). In addition, DNA cleavage bands were observed with dCs when the purified cross-linked products were heated in 1 M piperidine (Supporting Information, Figure S8). Collectively, these results showed that **1a**−**4a** alkylated dGs and dCs. Thus, the ICL could occur between dG and dC, two dGs, or two dCs in double-stranded DNA. This behavior is different from that of the quaternary ammonia salt **4b**, which

**Scheme 2. DNA Duplexes Used in This Study**

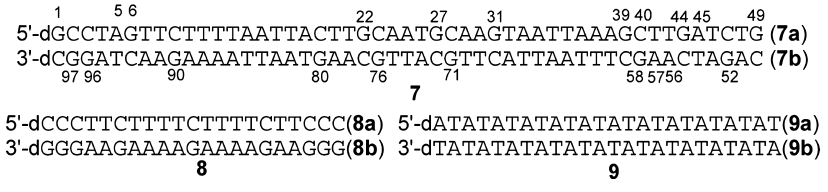



dx.doi.org/10.1021/jo401901x | J. Org. Chem. 2014, 79, 501−508

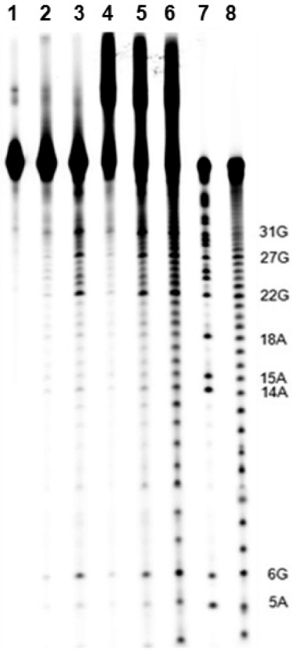


**Figure 2.** Determination of the reaction sites of **1a**. Phosphorimage autoradiogram of 20% denaturing PAGE analysis of the isolated ICL products and monoalkylated single-stranded DNA (**7a**′) upon heating in piperidine or phosphate buffer. The ICL product and **7a**′ were produced by incubation of duplex **7** with 1 mM **1a** and 1 mM $H_2O_2$. **7a** was radiolabeled at the 5′-terminus. Lane 1: isolated monoalkylated single stranded DNA (**7a**′). Lane 2: **7a**′ was heated in phosphate buffer at 90 °C for 30 min. Lane 3: **7a**′ was heated in 1.0 M piperidine at 90 °C for 30 min. Lane 4: the ICL was heated in phosphate buffer at 90 °C for 30 min. Lane 5: the ICL product was heated in 1.0 M piperidine at 90 °C for 30 min. Lane 6: Fe·EDTA treatment of ICL. Lane 7: G+A sequencing. Lane 8: Fe·EDTA treatment of **7**.

reacted mainly with dG, dA and dCs.[13] That is, the leaving group influenced both the cross-linking efficiency and the cross-linking site.

Around 50% of the ICLs were stable to piperidine treatment, which suggests that alkylations may also have occurred at the exocyclic amines of dG and dC to form heat-stable adducts. In addition, similar cleavage patterns were observed with single-stranded DNA, indicating monoalkylation or intrastrand cross-link formation (Supporting Information, Figures S3−S5). Furthermore, enzymatic digestion assay of the isolated ICL product and drug-treated single stranded DNA with snake-venom phosphodiesterase and alkaline phosphatase has been performed to acquire more detailed information about the cross-linking sites.

Enzyme-digested nucleotide mixtures were purified by HPLC and analyzed by mass spectroscopy (Figure 3). An obvious new peak with a retention time of ∼7.9 min was observed and accumulated in measurable quantities. It was characterized by LC−MS, which showed the exact mass of guanine-dC adduct **11** [**11** + H]$^+$ calcd 497.2, found 497.3) (Supporting Information, Figure S9). We propose that compound **11** might result from deglycosylation of the corresponding N7 adduct of dG (**10**). Rokita and co-workers showed that deglycosylation easily occurred with N7-alkylated dG leading to an N7 adduct of guanine.[12] Therefore, the cross-linking sites induced by **1a** most likely occurred at dGs and dCs. Similarly, an adduct with a retention time of 7.8 min and a mass of 497.3 was observed with drug-treated single stranded DNA, which

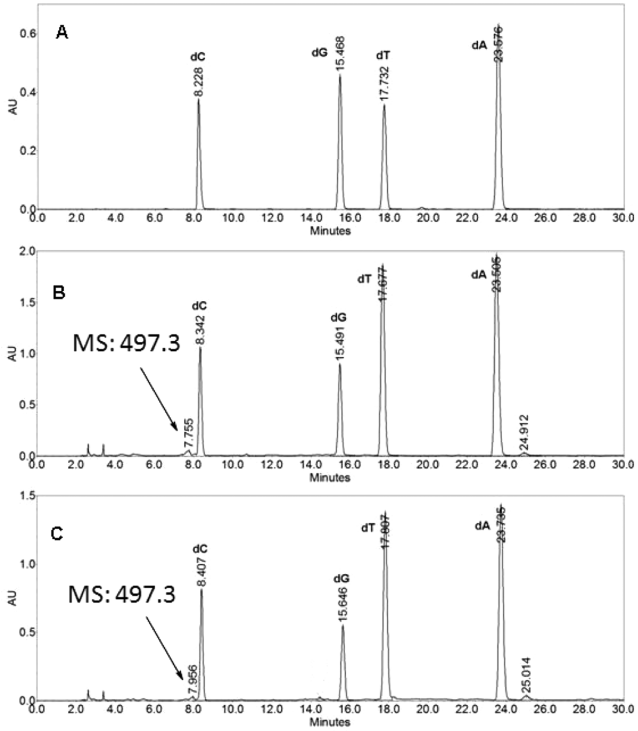


**Figure 3.** HPLC profiles of the enzymatic analysis: (A) DNA duplex **7** only as control; (B) **1a**-treated single-stranded **7a** and **7b**; (C) ICL products induced by **1a**, obtained by digestion with snake venom phosphodiesterase followed by alkaline phosphatase (analyzed by reversed-phase HPLC (RP-18, at 260 nm) using gradient: 0−30 min 2−20% MeOH in water, 30−35 min 20−50% MeOH in water, 35−42 min 50−100% MeOH in water, 42−50 min 100% MeOH in water, at a flow rate 1.0 mL/min).

indicated that intrastrand cross-linking took place between dGs and dCs too. Although we have tried to synthesize an authentic sample of **11** by reacting **1a** with dG and dC, we could not succeed in any of our efforts in isolation of these adducts from the monomer reactions. However, we observed that other alkylating agents formed N7-alkylated dG which decomposed to N7-alkylated guanine (unpublished data).

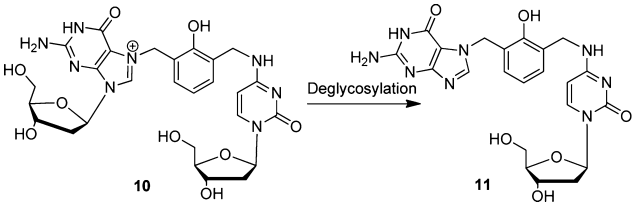


Next, we determined the rate constants for ICL formation induced by **1a**−**3a**, **4b**, and **4c** (Table 1). For all compounds, ICL growth followed first-order kinetics (Supporting Informa-

**Table 1. Rate of ICL Growth from 7 upon Treatment with Bromides and Salts**

| compd | $k_{obs}$, $10^{-5}$ $s^{-1}$ | $t_{1/2}$, min |
|---|---|---|
| **1a** | 8.8 ± 1.3 | 130 ± 13 |
| **2a** | 14.1 ± 1.5 | 82 ± 8 |
| **3a** | 13.8 ± 1.2 | 84 ± 9 |
| **4b** | 4.9 ± 0.5 | 234 ± 9 |
| **4c** | 3.7 ± 0.3 | 312 ± 10 |


dx.doi.org/10.1021/jo401901x | J. Org. Chem. 2014, 79, 501−508

tion, Figure S10). The rate constants for bromides **1a**−**3a** were 2−3 times the rate constant for quaternary ammonium salt **4b**.[13] This indicated that better leaving groups facilitate the QM formation.[21] Surprisingly, the cross-link yields (**4c** > **4b** ≈ **1a** ≈ **2a** > **3a**) do not correlate well with the kinetics (**2a** ≈ **3a** > **1a** > **4b** ≈ **4c**). Bromides **1a**−**3a** showed a larger *k* but a lower ICL yield than the salt **4b** or **4c**. One of the possible reasons is that the better leaving properties of −Br lead to nucelophilic substitution of bromides **1a**−**3a** by water under the reaction conditions. The NMR analysis of **1a**−**3a** in a mixture of DMSO and deuterated phosphate buffer (10:1) without addition of $H_2O_2$ showed formation of the hydrolysis intermediates (Supporting Information, Figures S11B, 12B, and 13B). The degree of the bromide hydrolysis increased with an increase in the percentage of water. To ensure all compounds were soluble in a mixture of DMSO and phosphate buffer, we could use a maximum of 9% buffer. Finally, a solvent mixture of 10:1 DMSO/buffer was used for NMR measurements. The hydrolysis of compounds **1a**−**3a** can be seen from the appearance of a variety of new peaks in the region between 4.0 and 6.0 ppm. However, this was not observed with **4b** (Supporting Information, Figure S14B). Our recent studies about the substituent effects on QM formation also indicated that both boronate ester and the benzylic bromo group were easily hydrolyzed to generate (2-(hydroxymethyl)phenyl)-boronic acid derivatives, which underwent intramolecular esterification to form benzo[*c*][1,2]oxaborol-1(3*H*)-ol derivatives (**A**).[21] In addition, bromides could be directly oxidized by excess $H_2O_2$, leading to 1,2-dihydroxybenzene derivatives (**B**). However, this phenomenon was not observed with the corresponding quaternary ammonium salts.[21] In summary, both hydrolysis and oxidization reaction of bromide analogues might lead to the lower DNA ICL yields.

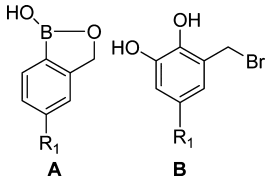


Considering that compound **4c** also contains one bromo group but led to the highest ICL yield, we fully investigated the effect of other factors, such as the mechanism and the kinetics of the QM generation, on the ICL formation. We propose that the mechanism of ICL formation induced by **1a**−**4a** and **4c** is similar to that for **4b**:[13] that is, **1a**−**4a** or **4c** react with $H_2O_2$ to form phenol intermediates, which directly cross-link DNA via QMs (Scheme 4 and Supporting Information, Scheme S1). However, owing to the instability and high reactivity of the phenol intermediates, they were not isolated from the reaction mixtures. NMR analysis of the reaction of **1a** with $H_2O_2$ showed a variety of new peaks in the region between 4.0 and 6.0 ppm (Supporting Information, Figure S15). As described previously, the phenol products generated from the arylboronates having −Br as a leaving group quickly form QMs which react with various nucleophiles or the phenol analogues which could be oxidized by excess $H_2O_2$ leading to 1,2-dihydroxybenzene derivatives (**B**).[21] To confirm fast QM formation from **1a**, we performed a QM-trapping experiment with a large excess of ethyl vinyl ether (EVE). When **1a** was incubated at 37 °C for 24 h in the presence of $H_2O_2$ and EVE, QM−EVE adduct **12** was generated (Scheme 5A). In contrast, the reaction of **1b** with $H_2O_2$ produced stable phenol product **1e**, which was isolated in quantitative yield (Scheme 5C and Supporting Information, Figure S16). Furthermore, no QM−EVE adduct was detected from the reaction of **1e** with EVE. This result is consistent with the results of the cross-linking study.

Similarly, QM−EVE adducts **13**−**15** were obtained from QM-trapping reactions of bromides **2a**−**4a** (Scheme 5B). This result indicated that the phenol intermediates generated by the reactions of **2a**−**4a** with $H_2O_2$ efficiently formed QMs under physiological conditions. Unlike the reactions of **2a** and **3a**, the reactions of **2b** and **3b** with $H_2O_2$ yielded stable phenol products that did not undergo QM formation.[13] In addition, the QM−EVE adduct **15** was formed from **4a**, **4b**, and **4c**. The reaction of **4b** and **4c** containing trimethyl amine leaving group with EVE took more than 48 h, whereas the QM-trapping reaction of **4a** was complete within 3 h. All these results indicated that the bromo leaving group greatly facilitated $H_2O_2$-induced QM formation from the arylboronates. Different from **1b**−**3b**, compounds **4b** and **4c** produced QMs even though they contain the poor leaving group ($NMe_3$). As previously described, the reaction of bisboronates **4b** and **4c** with $H_2O_2$ induced two electron-donating groups (OH) to the benzene ring (see **4e**) (Scheme 4c).[13] The addition of the second donating group facilitated QM formation from **4e**.[13]

In order to determine whether formation of the phenol intermediates or QM generation is the rate-determining step for DNA ICL formation, the reaction of these compounds with $H_2O_2$ was monitored by NMR analysis (Supporting Information, Figure S11−14, S17, and S18). Due to the poor solubility of boronate esters in $D_2O$, all compounds were hydrolyzed to the corresponding boronic acids in DMSO/phosphate buffer (10:1) prior to the addition of $H_2O_2$. Then, more $D_2O$ was added to reach a condition which was similar to the DNA cross-linking condition. However, if the ratio of phosphate buffer to DMSO was more than 2:3, the boronic acids also precipitated out. Finally, we used a mixture of phosphate buffer/DMSO (2:3) for the kinetic study. From the disappearance of the peaks at about 5.0 ppm (peak **d**), we were able to figure out the relative rate for the phenol intermediate formation. The relative reaction rates of these compounds with $H_2O_2$ are in the order of **4a** ≈ **4b** ≈ **4c** ≥ **3a** > **1a** > **2a** (Table 2, Supporting Information, Figure S19). The reactions of diboronates **4a**−**c** were too fast to determine the rate constant by NMR under these conditions (Supporting Information, Figures S14D−E, S17D−E, and S18C−D). The relative rates of QM formation were estimated by the formation of the final products (peak **f**, its hydrolyzed compounds or peak **f′**, the formed free $NMe_3$), which showed the following trend: **4a** > **3a** > **1a** > **2a** ≥ **4b** ≈ **4c** (Table 2, Supporting Information, Figure S19). The kinetic data for DNA ICL formation (**2a** ≈ **3a** > **1a** > **4b** ≈ **4c**) (Table 1) showed a trend similar to those for QM formation but different from those for formation of the phenol intermediates (Figure 4), which suggested that QM formation is the rate-limiting step for DNA cross-linking. For **4c** with a mixed leaving group −Br and $NMe_3$, departure of $NMe_3$ is the rate-determining step which took about 40 h while departure of −Br occurred within 3 min (Supporting Information, Figure S17).

Among the four bromide analogues, **1a** and **2a** showed ICL yields that were 3 times the ICL yield from **3a** and 9 times that from **4a**. Compound **4c** with a mixed leaving group −Br and $NMe_3$ proved to be the most efficient for inducing ICL formation. We propose another two possible explanations for the greater cross-linking efficiency of **1a**, **2a**, and **4c**: (1) better


dx.doi.org/10.1021/jo401901x | *J. Org. Chem.* 2014, 79, 501−508

**Scheme 4. Mechanism of $H_2O_2$-Induced QM Generation and ICL Formation by 1a, 2a, and 4c**

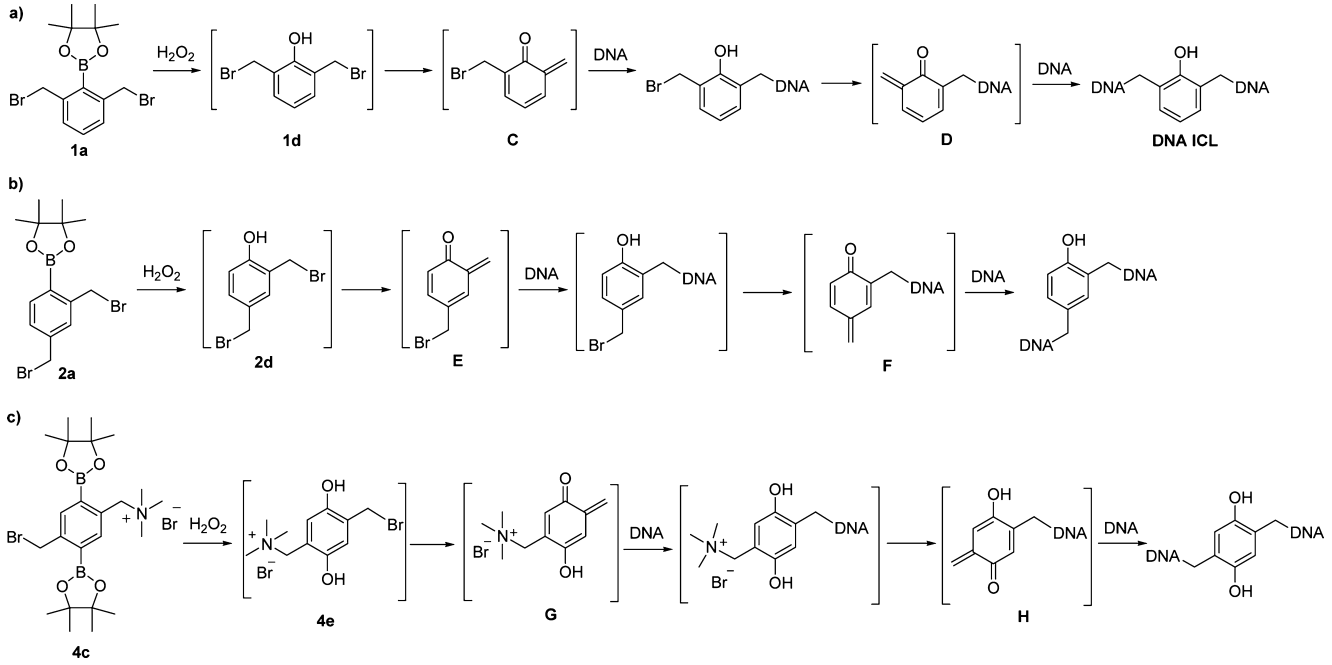


**Scheme 5. Effect of the Leaving Group on QM Formation**[a]

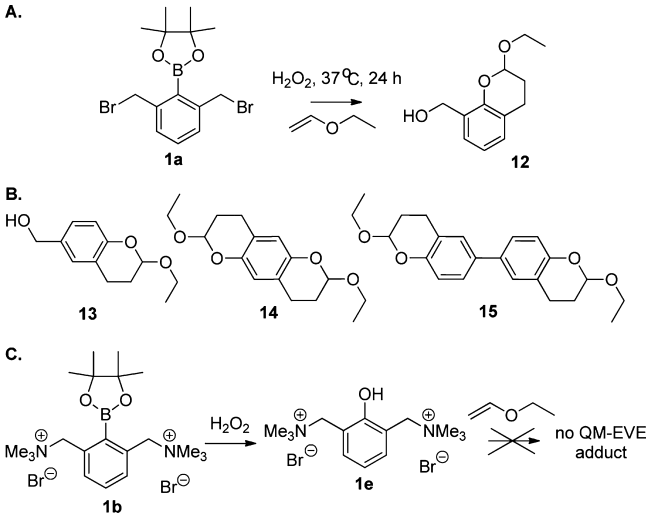


[a](A) QM-trapping product **12** was generated by reaction of **1a**, $H_2O_2$, and EVE. (B) QM-trapping products **13**–**15** were generated from **2a**–**4a**. (C) no QM-EVE adduct was generated from quaternary ammonia salt **1b**. Phenol product **1e** was obtained instead.

**Table 2. Rate of Starting Material Disappearance and QM Formation**

| | disappearance of starting materials | | QM formation | |
|---|---|---|---|---|
| compd | time of completion (min) | $k_{obs}$ ($10^{-5}$ $s^{-1}$) | time of completion (min) | $k_{obs}$ ($10^{-5}$ $s^{-1}$) |
| **1a** | 60 | 39.0 ± 1.5 | 60 | 9.5 ± 0.2 |
| **2a** | 90 | 36.7 ± 3.8 | 90 | 12.2 ± 1.1 |
| **3a** | 30 | 77.0 ± 2.1 | 30 | 20.0 ± 4.0 |
| **4a** | <3 | nd | <3 | nd |
| **4b** | <3 | nd | ~3000 | 4.6 ± 0.3 |
| **4c** | <3 | nd | ~2400 | 4.8 ± 0.5 |

[a]nd: not determined.

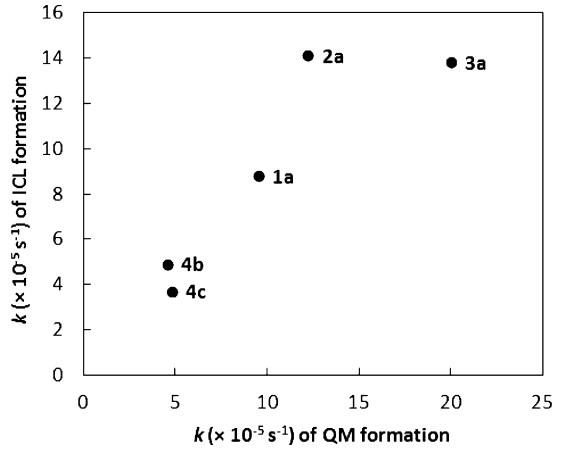


**Figure 4.** Relationship between the rate constant ($k$) of ICL formation ($y$-axis) and that of QM formation ($x$-axis).

water solubility and (2) stepwise generation of bisQMs from the corresponding phenol derivatives (Scheme 4). Compounds **1a**, **2a**, and **4c** were much more soluble than **3a** and **4a** under the reaction conditions tested. Furthermore, the two quinone methides (**C**, **D** or **E**, **F**) were generated from **1a** or **2a** in a stepwise process (Scheme 4). Once the first QM (**C** or **E**) reacted with one DNA strand, the stepwise formed second QM (**D** or **F**) would have better interaction with the nucleophilic centers in the complementary DNA strand, which resulted in more efficient DNA ICL formation. For **4c**, the fast formation of the first QM (**G**) plays an important role for its higher ICL yield than compound **4b**. In contrast, the reaction of **3a** likely generated two methide groups simultaneously (Scheme S1A, Supporting Information), in which case only molecules that were already well-positioned between two nucleophilic centers of two DNA strands would generate DNA ICLs, and the ICL yield would drop if either of the two methide groups reacted


dx.doi.org/10.1021/jo401901x | J. Org. Chem. 2014, 79, 501–508

with $H_2O$ prior to addition of a nucleophile from the DNA duplex.[24] However, we cannot exclude other explanations for the greater cross-linking efficiency of **1a**, **2a**, and **4c**, such as DNA sequence, molecular structure, or distance between cross-linking sites.

The crystal structures of bromides **1a**−**4a** suggest that they could easily enter the minor or major groove of DNA (Figure 5

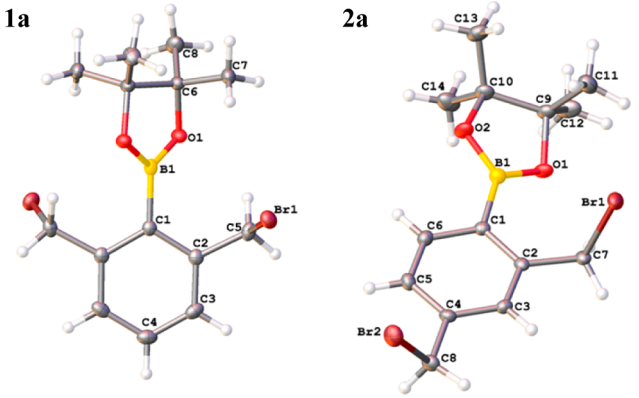


**Figure 5.** X-ray crystal structures of **1a** and **2a**.

and Supporting Information, and Figures S38 and S39). For example, the distance between B1A and B2A for the largest molecule (**3a**) is 10.2 Å; comparatively, the widths of the DNA minor groove and the major groove are 12 Å and 22 Å respectively. Thus, these molecules can interact with DNA either through minor groove or major groove. The bromomethylene groups extended almost perpendicularly from the central benzene ring like two arms and were in a *syn* orientation for **2a** and **3a** and an *anti* orientation for **1a** and **4a**. This result indicates that the C−Br bonds could freely rotate. The distances between the two methide groups were 5.1 Å for **1a**, 5.0 Å for **2a**, 8.6 Å for **3a**, and 5.8 Å for **4a**. In addition, the two central benzene rings in **3a** were rotated relative to each other at a torsion angle C2−C1−C14−C19 of 44.9(7)°. This angle results in a more flexible spatial conformation. Overall, the medium size, the structural flexibility, and the medium distance between the two formed methide groups make all these molecules suitable for interaction with DNA duplexes to form ICLs.

## CONCLUSIONS

In summary, our investigation of $H_2O_2$-induced reactions of nine arylboronate esters with DNA revealed that the benzylic leaving group and the aromatic core structure significantly affected the DNA cross-linking ability of the arylboronates. The mechanism of ICL formation induced by these arylboronates involves generation of phenol intermediates which directly produce QMs capable of cross-linking DNA. The QM formation is the rate-determining step for DNA cross-linking. Bromine, the better of the two leaving groups, facilitated the efficient generation of QMs. Meanwhile, the core structure determined whether bisQM formation was stepwise or simultaneous, which greatly altered the cross-linking ability of the bisQMs. More importantly, incorporation of mixed leaving groups such as Br and $NMe_3$ greatly enhances the DNA cross-linking efficiency. Overall, our results suggest an effective strategy for designing promising anticancer drugs that release QMs upon activation by ROS in vivo. Our findings may also be useful for designing novel arylboronic esters that can serve as ROS biosensors and other applications in medicine and chemical biology.

## EXPERIMENTAL SECTION

**General Methods.** All chemicals were commercially purchased and used without further purification. Thin-layer chromatography (TLC) was carried out on precoated silica gel plates and visualized under UV light. Oligonucleotides were synthesized via standard automated DNA synthesis techniques. Deprotection of the synthesized DNA was carried out under mild deprotection conditions (28% aq $NH_3$, room temperature, overnight). Oligonucleotides were purified by 20% denaturing polyacrylamide gel electrophoresis. Radiolabeling was carried out according to the standard protocols. Quantification of radiolabeled oligonucleotides was carried out using a Molecular Dynamics Phosphorimager equipped with ImageQuant Version 5.1 software. Enzymatic digestion products were purified with a HPLC, and mass spectra were available on an electron spray injection mass Spectrometer (ESI). $^1H$, $^{13}C$ NMR spectra were collected on 300 and 500 MHz FT-NMR spectrometers. High-resolution mass spectrometry was carried out on an atmospheric-pressure chemical ionization (APCI) TOF mass spectrometer. X-ray crystallography was performed on a diffractometer and crystal structures were solved with the Olex2 software.

**2-(2,6-Bismethylphenyl)-4,4,5,5-tetramethyl[1,3,2]-dioxaborolane (6).** 2-Bromo-1,3-dimethyl-benzene (**5**: 0.74 g, 4 mmol), bis(pinacolato)diboron (1.53 g, 6 mmol), KOAc (1.18 g, 12 mmol), and $PdCl_2$(dppf) (98 mg, 0.12 mmol) were dissolved in DMF (40 mL) under argon atmosphere. The mixture was heated at 85 °C for 48 h and cooled to room temperature. Then, water (100 mL) was added, and the mixture was extracted with $CH_2Cl_2$ (3 × 50 mL). The combined organic layer was washed with water and brine, dried over anhydrous $Na_2SO_4$, and filtrated, and the solvent was evaporated. The crude product was purified through column chromatography with 0−50% EtOAc in hexane to provide **6** as colorless oil (0.74 g, 80%): $^1H$ NMR (300 MHz, $CDCl_3$) $\delta$ 7.13 (t, $J$ = 7.0 Hz, 1H), 6.95 (d, $J$ = 7.0 Hz, 2H), 2.42 (s, 6H), 1.41 (s, 12H); $^{13}C$ NMR (500 MHz, $CDCl_3$) $\delta$ 141.6, 129.1, 126.4, 83.4, 24.9, 22.2. The NMR spectra were consistent with literature values.[25]

**2-(2,6-Bisbromomethylphenyl)-4,4,5,5-tetramethyl[1,3,2]-dioxaborolane (1a).** Compound **6** (0.83 g, 3.6 mmol) was dissolved in $CH_3CN$ (55 mL), and NBS (1.6 g, 9 mmol) and AIBN (62.9 mg) were added. The mixture was refluxed at 90 °C for 3 h. Then the mixture was concentrated and dissolved in DCM (100 mL). The organic phase was washed with $H_2O$ (3 × 50 mL) and dried with anhydrous $Na_2SO_4$. The solution was evaporated, and the residue was subjected to column chromatography on silica gel with 0−50% DCM in hexane to give **1a** as a white solid (0.7 g, 50%): mp 159−163 °C; $^1H$ NMR (300 MHz, $CDCl_3$) $\delta$ 7.31 (m, 3H), 4.84 (s, 4H), 1.49 (s, 12H); $^{13}C$ NMR (500 MHz, $CDCl_3$) $\delta$ 144.4, 130.8, 130.0, 84.4, 34.0, 25.2; HRMS (EI) $m/z$ calcd for $C_{14}H_{19}BBr_2O_2$ $[M]^+$ 387.9845, found 387.9829. The NMR spectra were consistent with literature value.[25]

**1,1′-(2-(4,4,5,5-Tetramethyl[1,3,2]dioxaborolan-2-yl)-1,3-henylene)bis(*N*,*N*,*N*-trimethylmethanaminium) Bromide (1b).** Compound **1a** (0.182 g, 0.47 mmol) was suspended in $CH_3CN$ (10 mL), and 4.2 M trimethylamine (0.34 mL, 1.41 mmol) in ethanol was added dropwise with stirring. The reaction mixture was stirred at rt for 12 h and concentrated, resulting in **1b** as a white solid (0.22 g, 95%): mp 250−256 °C; $^1H$ NMR (300 MHz, $D_2O$) $\delta$ 7.73−7.70 (m, 3H), 4.79 (s, 4H), 3.05 (s, 18H), 1.41 (s, 12H); $^{13}C$ NMR (500 MHz, DMSO) $\delta$ 136.3, 135.0, 131.3, 85.9, 68.1, 52.9, 25.3; HRMS (ESI) $m/z$ calcd for $C_{20}H_{37}BBr_2N_2O_2$ $[(M - 2Br)/2]^+$ 174.1474, found 174.1460.

**1-(4-(Bromomethyl)-2,5-bis(4,4,5,5-tetramethyl-1,3,2-dioxaborolan-2-yl)phenyl)-*N*,*N*,*N*-trimethylmethanaminium Bromide (4c).** Bromide **4a** (50 mg, 0.1 mmol) was dissolved in $CH_3CN$ (2 mL), and 4.2 M trimethylamine (24 $\mu$L, 0.1 mmol) in ethanol was added dropwise with stirring. The reaction mixture was concentrated after 24 h at room temperature. The residue was purified by column chromatography with 0−15% methanol in DCM to afford


dx.doi.org/10.1021/jo401901x | J. Org. Chem. 2014, 79, 501−508

compound **4c** as a white solid (7 mg, 12%): mp 216−220 °C; $^1$H NMR (300 MHz, $CDCl_3$) $\delta$ 8.02 (s, 1H), 7.87 (s, 1H), 4.99 (s, 2H), 4.91 (s, 2H), 3.46 (s, 9H), 1.39 (s, 24H); $^{13}$C NMR (500 MHz, $CDCl_3$) $\delta$ 146.3, 140.6, 139.2, 131.8, 85.1, 84.7,68.3, 53.1, 32.3, 25.0, 24.9; HRMS (ESI) $m/z$ calcd for $C_{23}H_{39}B_2Br_2NO_4$ $[M - Br]^+$ 494.2243, found 494.2247.

**1,1′-(2-Hydroxy-1,3-phenylene)bis(*N,N,N*-trimethylmethanaminium) Bromide (1e).** A solution of **1b** (50 mg) in a mixture of $H_2O$ (3 mL), 1 M potassium phosphate buffer (52 $\mu$L, pH 8), and $H_2O_2$ (1.9 equiv of **1b**) was incubated at 37 °C for 3 h and then rinsed with ethyl acetate (3 × 5 mL) and DCM (3 × 5 mL). The aqueous phase was dried under vacuum yielding **1e** as a white solid quantitatively: mp 214−218 °C; $^1$H NMR (500 MHz, $D_2O$) $\delta$ 7.32 (d, $J$ = 7.5 Hz, 2H), 6.56 (t, $J$ = 7.5 Hz, 1H), 4.36 (s, 4H), 2.96 (s, 18H). $^{13}$C NMR (500 MHz, DMSO) $\delta$ 137.3, 118.2, 112.8, 65.6, 52.2; HRMS (ESI) $m/z$ calcd for $C_{14}H_{26}Br_2N_2O$ $[(M - 2Br)/2]^+$ 119.1017, found 119.1022.

**QM Trapping Assay. General Procedure.** A solution of bromides **1a**−**4a** (50 mg) in a mixture of $CH_3CN$ (3 mL) and 1 M potassium phosphate buffer (52 $\mu$L, pH 8) was incubated at 37 °C for 30 min with excess ethyl vinyl ether (EVE). Then $H_2O_2$ (1.9 equivalent of bromides) was added to initiate the reaction. The reaction mixture was stirred at 37 °C for 24 h and then evaporated. Water (2 mL) was added to the residue, and the resulting mixture was extracted with ethyl acetate (3 × 5 mL). The organic phase was combined, dried over anhydrous $Na_2SO_4$, and evaporated. The crude product was purified through column chromatography with 0−50% EtOAc in hexane to provide QM−EVE adducts **12**−**15**.

**(2-Ethoxychroman-8-yl)methanol (12):** colorless oil, 16% yield (4.9 mg); $^1$H NMR (300 MHz, $CDCl_3$) $\delta$ 7.20−6.82 (m, 3H), 5.35 (s, 1H), 4.78−4.58 (m, 2H), 3.98−3.84 (m, 1H), 3.72−3.58 (m, 1H), 3.05−2.88 (m, 1H), 2.68−2.56 (m, 1H), 2.28 (s, 1H), 2.12−1.92 (m, 2H), 1.21 (t, $J$ = 7.2 Hz, 3H); $^{13}$C NMR (500 MHz, $CDCl_3$) $\delta$ 150.1, 128.9, 128.5, 126.5, 122.6, 120.4, 97.2, 63.9, 62.0, 26.5, 20.5, 15.1; HRMS (APCI) $m/z$ Calcd for $C_{12}H_{16}O_3$ $[M - H]^+$ 207.1021, found 207.1025.

**(2-Ethoxychroman-6-yl)methanol (13):** colorless oil, 11% yield (3.4 mg); $^1$H NMR (300 MHz, $CDCl_3$) $\delta$ 7.16−7.08 (m, 2H), 6.82 (d, $J$ = 8.1 Hz, 1H), 5.27 (s, 1H), 4.61 (s, 2H), 3.98−3.84 (m, 1H), 3.72−3.58 (m, 1H), 3.08−2.92 (m, 1H), 2.72−2.58 (m, 1H), 2.12−1.92 (m, 2H), 1.61 (br, 1H), 1.21 (t, $J$ = 7.2 Hz, 3H). $^{13}$C NMR (500 MHz, $CDCl_3$): $\delta$ 151.9, 133.0, 128.5, 126.5, 122.7, 117.1, 97.0, 65.3, 63.7, 26.5, 20.5, 15.1; HRMS (APCI) $m/z$ calcd for $C_{12}H_{16}O_3$ $[M - H]^+$ 207.1021, found 207.1023.

**2,7-Diethoxy-2,3,4,7,8,9-hexahydropyrano[2,3-*g*]chromene (14):** colorless oil, 21% yield (8.8 mg); $^1$H NMR (300 MHz, $CDCl_3$) $\delta$ 6.54 (s, 2H) 5.21 (s, 2H), 3.96−3.86 (m, 2H), 3.72−3.58 (m, 2H), 3.04−2.90 (m, 2H), 2.64−2.54 (m, 2H), 2.08−1.90 (m, 4H), 1.21 (t, $J$ = 7.2 Hz, 6H); $^{13}$C NMR (500 MHz, $CDCl_3$) $\delta$ 145.8, 121.5, 116.5, 96.8, 63.5, 26.7, 20.5, 15.1; HRMS (APCI) $m/z$ calcd for $C_{16}H_{22}O_4$ $[M + NH_4]^+$ 296.1862, found 296.1861.

**2,2′-Diethoxy-6,6′-bichroman (15):** colorless oil, 26% yield (13.8 mg); $^1$H NMR (300 MHz, $CDCl_3$) $\delta$ 7.34−7.24 (m, 4H), 6.87 (d, 2H, J = 8.1 Hz), 5.30 (s, 2H), 3.98−3.88 (m, 2H), 3.72−3.62 (m, 2H), 3.08−2.96 (m, 2H), 2.74−2.62 (m, 2H), 2.08−1.92 (m, 4H), 1.21 (t, J = 7.2 Hz, 6H); $^{13}$C NMR (500 MHz, $CDCl_3$) $\delta$ 151.3, 133.7, 127.6, 125.7, 122.7, 117.2, 97.0, 63.7, 26.6, 20.7, 15.2; HRMS (APCI) $m/z$ calcd for $C_{22}H_{26}O_4$ $[M + NH_4]^+$ 372.2175, found 372.2178.

**Interstrand Cross-Link Formation and Kinetics Study with Duplex DNA.** The $^{32}$P-labeled oligonucleotide (0.5 $\mu$M) was annealed with 1.5 equiv of the complementary strand by heating to 65 °C for 3 min in a buffer of 10 mM potassium phosphate (pH 7) and 100 mM NaCl, followed by slow cooling to room temperature overnight. The $^{32}$P-labeled oligonucleotide duplex (0.5 $\mu$M, 2 $\mu$L) was mixed with 1 M NaCl (2 $\mu$L), 100 mM potassium phosphate (2 $\mu$L, pH 8.0), 10 mM $H_2O_2$ (2 $\mu$L), compounds **1b**−**4b** (concentration range: 10 $\mu$M to 7 mM), and an appropriate amount of autoclaved distilled water to give a final volume of 20 $\mu$L. For Bromides **1a**−**4a**, 6 $\mu$L $CH_3CN$ was added in the reaction mixture to facilitate their dissolution. The reaction was incubated at 37 °C for 24 h, quenched by an equal volume of 90% formamide loading buffer, and then subjected to 20% denaturing polyacrylamide gel analysis. For kinetics study, aliquots (final concentration: 50 nM $^{32}$P-labeled oligonucleotide duplex, 100 mM NaCl, 10 mM potassium phosphate, 1 mM $H_2O_2$, 2 mM of **1**−**4**) were taken at the prescribed times, immediately quenched by 90% formamide loading buffer, and stored at −20 °C until being subjected to 20% denaturing PAGE analysis.

**Enzyme Digestion of Cross-Linked Oligonucleotides.** Interstrand cross-linked oligonucleotide (38 nmol) was dissolved in 0.1 M Tris−HCl buffer, pH 8.0 (300 $\mu$L) and snake-venom phosphodiesterase (8.0 $\mu$L, 0.34 U) in a buffer of 110 mM Tris−HCl, pH 8.9, 110 mM NaCl, 15 mM $MgCl_2$, and 50% glycerol was added. The mixture was incubated at 37 °C for 1 h. Then alkaline phosphatase (8.0 $\mu$L, 80 U) in 16 $\mu$L of alkaline phosphatase buffer (100 mM NaCl, 50 mM Tris−HCl, 10 mM $MgCl_2$ and 1 mM dithiothreitol) was added. The reaction mixture was incubated at 37 °C for another 1 h. The digested products were passed through a Microcon cellulose filter (10000 molecular cutoff, Amicon, Inc.) by centrifugation at 15000 rpm. The filtrate was collected, lyophilized, redissolved in $H_2O$ (500 $\mu$L), and analyzed by reversed-phase HPLC (RP-18, at 260 nm) using the following gradient: 0−30 min 2−20% MeOH in water, 30−35 min 20−50% MeOH in water, 35−42 min 50−0% MeOH in water, 42−50 min 0% MeOH in water, at a flow rate 1.0 mL/min.

**Stability Study of ICL Product Formed with DNA Duplex.** After the cross-linking reaction, the reaction mixtures (0.35 $\mu$M DNA duplex, 20 $\mu$L) were coprecipitated with calf thymus DNA (2.5 mg/mL, 5 $\mu$L) and NaOAc (3 M, 5 $\mu$L) in the presence of EtOH (90 $\mu$L) at −80 °C for 30 min, followed by centrifuging for 5 min at 15000 rmp. The supernatant was removed, and the pellet was washed with cold 75% EtOH and lyophilized for 30 min in a Centrivap Concentrator of LABCONCO at 37 °C. The dried DNA fragments were dissolved in $H_2O$ (30 $\mu$L) and divided into three portions. One portion (10 $\mu$L) was incubated with piperidine (2 M, 10 $\mu$L) at 90 °C for 30 min, and the second portion (10 $\mu$L) was incubated with 0.1 M NaCl and 10 mM potassium phosphate buffer (pH 8, 10 $\mu$L) under the same conditions, and the third portion was used as control sample. The samples were subjected to electrophoresis on a 20% denaturing polyacrylamide gel.

**Hydroxyl Radical Reaction (Fe·EDTA Reaction).** Fe(II)·EDTA cleavage reactions of $^{32}$P-labeled oligonucleotide (0.1 $\mu$M) were performed in a buffer containing 50 $\mu$M $(NH_4)_2Fe(SO_4)_2$, 100 $\mu$M EDTA, 5 mM sodium ascorbate, 0.5 M NaCl, 50 mM sodium phosphate (pH 7.2), and 1 mM $H_2O_2$ for 3 min at room temperature (total substrate volume 20 $\mu$L) and then quenched with 100 mM thiourea (10 $\mu$L). Samples were lyophilized and incubated with 1 M piperidine (20 $\mu$L) at 90 °C for 30 min. The mixture was lyophilized again, dissolved in 20 $\mu$L $H_2O$: 90% formamide loading buffer (1:1), and subjected to 20% denaturing PAGE analysis.

## ■ ASSOCIATED CONTENT

### Supporting Information

Copies of $^1$H and $^{13}$C NMR spectra for compounds **1a,b**, **4c**, **10b**, and **12**−**15**, DNA experiments, NMR analysis, and X-ray crystal structures and analysis data of **1a**−**4a**. This material is available free of charge via the Internet at http://pubs.acs.org.

## ■ AUTHOR INFORMATION


### Corresponding Author

*E-mail: pengx@uwm.edu.

### Author Contributions

‡These authors contributed equally to this work.


### Notes

The authors declare no competing financial interest.

## ■ ACKNOWLEDGMENTS

This work was supported by the National Cancer Institute (1R15CA152914-01), Great Milwaukee Foundation (Shaw

Scientist Award), and UWM Research Growth Initiative (RGI101X234).

## REFERENCES

(1) Huang, P.; Feng, L.; Oldham, E. A.; Keating, M. J.; Plunkett, W. *Nature* **2000**, *407*, 390−395.
(2) Raj, L.; Ide, T.; Gurkar, A. U.; Foley, M.; Schenone, M.; Li, X.; Tolliday, N. J.; Golub, T. R.; Carr, S. A.; Shamji, A. F.; Stern, A. M.; Mandinova, A.; Schreiber, S. L.; Lee, S. W. *Nature* **2011**, *475*, 231−234.
(3) Trachootham, D.; Alexandre, J.; Huang, P. *Nature Rev.* **2009**, *8*, 579−591.
(4) Peng, X.; Gandhi, V. *Ther. Delivery* **2012**, *7*, 823−833.
(5) Szatrowski, T. P.; Nathan, C. F. *Cancer Res.* **1991**, *51*, 794−798.
(6) Lim, S. D.; Sun, C.; Lambeth, J. D.; Marshall, F.; Amin, M.; Chung, L.; Petros, J. L.; Arnold, R. S. *Prostate* **2005**, *62*, 200−207.
(7) Hileman, E. O.; Liu, J.; Albitar, M.; Keating, M. J.; Huang, P. *Cancer Chemother. Pharmacol.* **2004**, *53*, 209−219.
(8) Kuang, Y.; Balakrishnan, K.; Gandhi, V.; Peng, X. *J. Am. Chem. Soc.* **2011**, *133*, 19278−19231.
(9) Wang, P.; Song, Y.; Zhang, L.; He, H.; Zhou, X. *Curr. Med. Chem.* **2005**, *12*, 2893−2913.
(10) Freccero, M. *Mini-Rev. Org. Chem.* **2004**, *1*, 403−415.
(11) Weinert, E. E.; Dondi, R.; Colloredo-Melz, S.; Frankenfield, K. N.; Mitchell, C. H.; Freccero, M.; Rokita, S. E. *J. Am. Chem. Soc.* **2006**, *128*, 11940−11947.
(12) Veldhuyzen, W. F.; Lam, Y. F.; Rokita, S. E. *Chem. Res. Toxicol.* **2001**, *14*, 1345−1351.
(13) Cao, S.; Wang, Y.; Peng, X. *Chem.—Eur. J.* **2012**, *18*, 3850−3854.
(14) Antonio, M. D.; Doria, F.; Mella, M.; Merli, D.; Profumo, A.; Freccero, M. *J. Org. Chem.* **2007**, *72*, 8354−8360.
(15) Verga, D.; Nadai, M.; Doria, F.; Percivalle, C.; Antonio, M. D.; Palumbo, M.; Richter, S. N.; Freccero, M. *J. Am. Chem. Soc.* **2010**, *132*, 14625−14637.
(16) Percivalle, C.; Rosa, A. L.; Verga, D.; Doria, F.; Mella, M.; Palumbo, M.; Antonio, M. D.; Freccero, M. *J. Org. Chem.* **2011**, *76*, 3096−3106.
(17) Hong, I. S.; Greenberg, M. M. *J. Am. Chem. Soc.* **2005**, *127*, 10510−10511.
(18) Veldhuyzen, W. F.; Pande, P.; Rokita, S. E. *J. Am. Chem. Soc.* **2003**, *125*, 14005−14013.
(19) Richter, S. N.; Maggi, S.; Mels, S. C.; Palumbo, M.; Freccero, M. *J. Am. Chem. Soc.* **2004**, *126*, 13973−13979.
(20) Van De Water, R. W.; Pettus, T. R. R. *Tetrahedron* **2002**, *58*, 5367−5405.
(21) Cao, S.; Christiansen, R.; Peng, X. *Chem.—Eur. J.* **2013**, *19*, 9050−9058.
(22) Haraguchi, K.; Delaney, M. O.; Wiederholt, C. J.; Sambandam, A.; Hantosi, Z.; Greenberg, M. M. *J. Am. Chem. Soc.* **2002**, *124*, 3263−3269.
(23) Peng, X.; Hong, I. S.; Li, H.; Seidman, M. M.; Greenberg, M. M. *J. Am. Chem. Soc.* **2008**, *130*, 10299−10306.
(24) Peng, H.; Wahi, M. S.; Rokita, S. E. *Angew. Chem., Int. Ed.* **2008**, *47*, 1291−1293.
(25) Lux, C. G.; Joshi-Barr, S.; Nguyen, T.; Mahmoud, E.; Schopf, E.; Fomina, N.; Almutairi, A. *J. Am. Chem. Soc.* **2012**, *134*, 15758−15764.